A Tap-Changing Algorithm for the Implementation of "Sen" Transformer

M. Omar Faruque, *Student Member, IEEE*, and Venkata Dinavahi, *Member, IEEE*

Abstract—**The "Sen" transformer (ST) is made out of a transformer and tap changers and is capable of regulating the active and the reactive power flow selectively in an electric transmission line. This paper focuses on the development of a novel algorithm capable of selecting the best combination of tap-settings for the compensating windings of the ST. Digital simulation model of the ST including a detailed tap-changer model has been developed in the PSCAD/EMTDC software package. The tap-changing algorithm of the ST has been implemented through a FORTRAN code that is interfaced with the rest of the model. Should there be any change in the magnitude of the compensating voltage and its phase angle, the tap-positions are readjusted accordingly. The results obtained from the simulation of the ST are compared with the simulation results of the UPFC which is a power electronics-based power-flow controller. The comparison shows good agreement between the results and hence validates the effectiveness of the proposed algorithm and the performance of the ST.**

Index Terms—**Flexible ac transmission systems (FACTS), modeling, simulation, "Sen" transformer (ST), unified power-flow controller (UPFC).**

I. INTRODUCTION

FLEXIBLE AC transmission systems (FACTS) have been developed for better control of electric power flow through the efficient utilization of existing transmission lines. In its most exotic form, the unified power-flow controller (UPFC) is a FACTS controller consisting of power-electronic components that can be employed for controlling the magnitude and phase angle of the line voltage and the line impedance simultaneously [1]–[3]; the concept of a shared dc link between a shunt and series connected converter was first introduced in the active power-line conditioner (APLC) [4], [5]. However, excessive installation and operating costs do not justify widespread use of such a controller. To address this issue, the "Sen" transformer (ST) was introduced [6]. The ST uses time-tested components, such as transformers and tap changers, and injects a voltage of variable magnitude and phase angle, such as a UPFC, in series with the transmission line, thereby regulating the active and reactive power flow in the line independently. Although the power circuit of the UPFC is capable of subcycle response, the adjustable responses of currently installed UPFCs are set in the
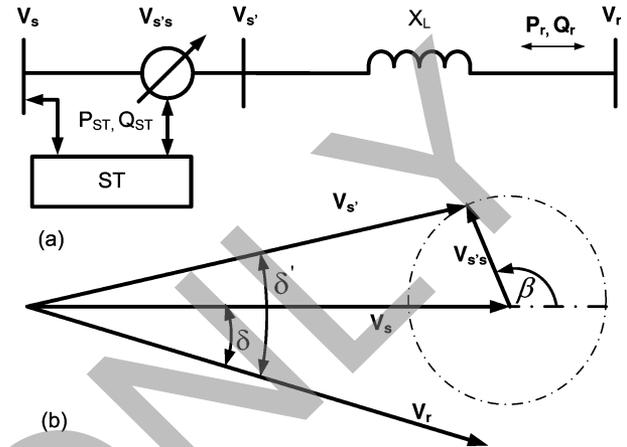
Fig. 1. (a) Transmission line with "ST" block. (b) Phasor diagram.

range of tens of line cycles and slower, thereby not utilizing the full speed response capability of the power electronic converter. In most power systems applications, the response of mechanical tap-changers in the range of seconds is quite acceptable.

Fig. 1(a) shows a transmission line on which the active and reactive power flows, P_r and Q_r are governed by the following equations:

$$P_r = \frac{V_s V_r}{X_L} \sin \delta \tag{1}$$

$$Q_r = \frac{V_s V_r}{X_L} \left(\cos \delta - \frac{V_r}{V_s} \right) \tag{2}$$

where V_s is the magnitude of the sending-end voltage, V_r is the magnitude of the receiving-end voltage, δ is the difference in phase angle between the sending-end and the receiving-end voltages, and X_L is the reactance of the line. By changing any of these parameters, both active and reactive power flow can be regulated. Fig. 1(b) shows the phasor diagram, where a series voltage $V_{s's}$, from an ST is added to the phase voltage V_s at an angle, β (leading), to produce the resultant voltage $V_{s'}$ which is at an angle δ' with respect to V_r. The angle β can be varied between $0°$ and $360°$.

A comparative study between digital simulation results of the ST and the UPFC has been carried out in [7] to show that the ST performs the essential power-flow regulating functions of the UPFC in a cost effective way. In practice, the implementation and operation of the ST requires a tap-changing algorithm that can provide appropriate tap settings for the compensating windings under various load conditions. Due to the discrete nature of the taps, the resulting power-flow control with the ST is discrete, unlike the UPFC where it is continuous. Any given

$V_{s's}$ and β can be approximated using several tap combinations of the ST windings. Therefore, the ST tap-selection algorithm must identify the best tap-setting combination. Currently, such a tap-selection algorithm is not available in the literature.

The objective of this paper is to develop an algorithm that can identify the contributing compensating windings and their corresponding tap-positions following a load change. After the algorithm for the tap-changing criteria is established, a detailed digital simulation model of the ST is developed in the PSCAD/EMTDC software. The proposed tap-selection algorithm has been implemented through a FORTRAN code that is interfaced with the rest of the model. Applying the ST tap-selection algorithm, detailed simulation studies were performed and the system response under various operating conditions were observed, and compared with the performance of the UPFC. The transient response of the ST due to mechanical tap changing has also been studied.

The paper is organized as follows. Section II briefly describes the construction of the ST. Section III describes the algorithm to determine the required tap positions of the compensating windings. The implementation of the ST and its tap selection in PSCAD/EMTDC is described in Section IV. Section V presents results of the ST simulation in comparison with that of a UPFC, followed by conclusions in Section VI.

II. "SEN" TRANSFORMER

In a "Sen" transformer (ST), as shown in Fig. 2, there are two units: exciter unit and compensating-voltage unit. The exciter unit consists of three primary windings (A, B, and C) that are Y-connected and placed on each limb of a three-limb, single-core transformer. The three-phase transmission-line voltage (V_{sA}, V_{sB}, and V_{sC}) at the sending end is applied in shunt to the exciter unit. The compensating-voltage unit consists of nine secondary windings, three of which are placed on each limb of the core e.g., a1, a2, and a3 on the first limb, b1, b2, and b3 on the second limb, and c1, c2, and c3 on the third limb. The induced voltages from three windings that are placed on three different limbs are combined through series connection to produce the compensating voltage for injection in series with the transmission line, e.g., a1, b1, and c1 for injection in A-phase, a2, b2, and c2 for injection in B-phase, and a3, b3, and c3 for injection in C-phase. The number of active turns in the three windings can be varied with the use of on-load tap changers. As a result, the magnitudes of the components of the three 120° phase-shifted-induced voltages are varied and, therefore, the composite voltage $V_{s's}$, which is the phasor sum of the three induced voltages, becomes variable in magnitude and variable in phase angle in the range of 0° and 360°. It should be noted that each of a1, b2, and c3 is tapped at the same number of turns; each of b1, c2, and a3 is tapped at the same number of turns; each of c1, a2, and b3 is tapped at the same number of turns. However, the number of turns in the a1-b2-c3 set, b1-c2-a3 set, and c1-a2-b3 set can be different from each other.
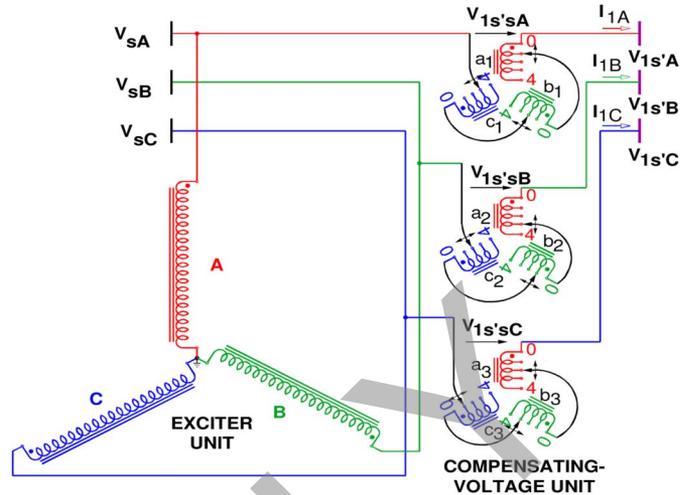
Fig. 2. Schematic diagram of "ST."

An ST connects a compensating voltage $V_{s's}$ of line frequency that is generated from the transformer's secondary windings connected in series. When connected in series with the transmission line, the compensating voltage of variable magnitude and variable angle modifies the magnitude and the angle of the sending-end voltage V_s to be the effective sending-end voltage $V_{s'}$ and, therefore, controls the active and reactive power flow in the transmission line independently.

ALGORITHM FOR SPLITTING THE COMPENSATING VOLTAGE INTO PHASOR COMPONENTS

The series compensating voltage $V_{s's}$ in any phase is derived from the contributions of the compensating windings of the ST from three different phases. If the phase angle of the series compensating voltage is exactly at 0°, 120° or 240°, it can be constructed from only one of the three phases a, c, or b, respectively. For any other angle, the series compensating voltage is constructed from two adjacent voltages.

Consider an ST, shown in Fig. 2, which has four tap positions in each of the nine compensating secondary windings. Each tap position provides a voltage of 0.1 p.u. and therefore, a maximum of 0.4 p.u. is obtained from each phase. The possible combinations of voltage tap-setting positions are shown by the dotted grid in Fig. 3(a). Let $V_{s's}$ be the required compensating voltage, at an angle β with reference to the corresponding phase angle. Then, one of the four combinations enclosed by the dashed circle must be selected. In addition, the selected combination must be the nearest to the voltage vector, $V_{s's}$. In Fig. 3(b) the circle is shown in an enlarged view, where the four combinations marked as 1, 2, 3, and 4 are vector distances r_1, r_2, r_3, and r_4, respectively, apart from the desired series voltage $V_{s's}$. These four vector distances indicate the error introduced due to the selection of any particular combination. Of the four distances, the one with the least magnitude, will introduce the least error and the corresponding tap-setting combination would be selected to construct $V_{s's}$. Let $V_{s's}^x$ and $V_{s's}^y$ denote the two rectangular components of $V_{s's}$ in the Cartesian coordinate system. Similarly, let $V_k{}^x$ and $V_k{}^y$ be the components of $V_k(k = 1, 2, 3, 4)$,
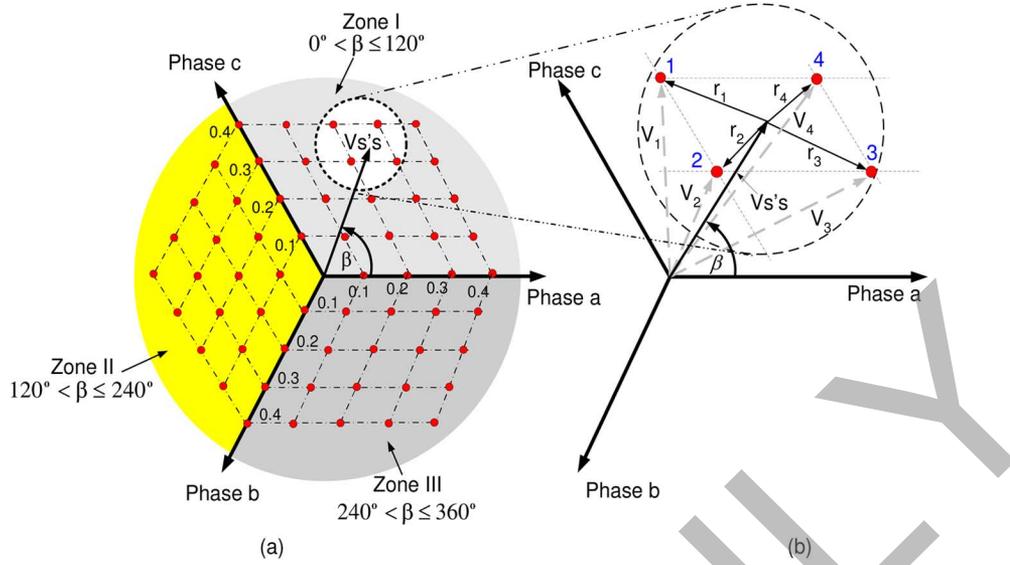
Fig. 3. (a) Tap position grid for the construction of $V_{s's}$. (b) Selection of the best tap setting.

formed by the four possible tap-setting combinations. Then, the error ε_k with respect to $V_{s's}$ is defined as

$$\varepsilon_k = \parallel r_k \parallel_2 = \sqrt{(V_k{}^x - V_{s's}^x)^2 + (V_k{}^y - V_{s's}^y)^2}. \quad (3)$$

The tap-setting combination corresponding to V_k with the smallest ε_k is selected as the best tap setting to implement $V_{s's}$. Thus, the algorithm to determine the best tap setting for $V_{s's}$ consists of the following steps.

Step 1) Get the input (magnitude, $V_{s's}$, and leading phase angle, β) about required series voltage injection in phase a.

Step 2) Based on β, identify the zone into which the series voltage phasor falls: Zone I $(0° < \beta \le 120°)$, Zone II $(120° < \beta \le 240°)$ and Zone III $(240° < \beta \le 360°)$. Next, identify the contributing (one or two) phase(s) and set the contribution of the other phase(s) to zero. When β is exactly equal to $0°, 60°, 120°, 180°, 240°,$ and $300°$ and the magnitude is exactly midpoint in between two consecutive grid positions, select the higher tap position.

Step 3) Based on the magnitude of $V_{s's}$, identify the four nearest tap-setting positions [dot positions on the grid in Fig. 3(a)].

Step 4) Calculate the normalized vector distances between voltages produced by these four tap positions and the compensating voltage, $V_{s's}$. This will give the magnitude of errors $\varepsilon_k (k = 1, 2, 3, 4)$ that would be introduced due to the selection of corresponding tap settings.

Step 5) Compare the errors and identify the tap-setting combination that yields the minimum error.

Step 6) Implement the tap setting in corresponding phase(s) in the ST through the use of load tap changers.

Step 7) Implement similar tap settings for voltages to be added in series with phases b and c.

TABLE I
DATA FOR THE ELECTRICAL SYSTEM AND THE ST

Parameters	Value
Base values	160 MVA and 138 kV
Sending end line-to-line voltage	$1\angle 0°$ p.u.
Receiving end line-to-line voltage	$1\angle -20°$ p.u.
Source impedance at the sending-end	1.0053 Ω and 19.17 mH
Transmission line impedance	3.0159 Ω and 59.19 mH
Rating of the ST transformer	30 MVA
Resistance and inductance of the ST	1.7854 Ω and 47.4 mH

Section IV describes how this algorithm has been implemented on the ST system.

III. MODELING OF "SEN" TRANSFORMER USING PSCAD/EMTDC

A digital computer simulation model of the ST has been developed using PSCAD/EMTDC v. 4.0.1. The model consists of two subsystems: the electrical subsystem (Fig. 4) and the tap-selection algorithm subsystem. Fig. 6 illustrates the interface between the two subsystems.

A. Electrical System

Fig. 4 shows the electrical system and the ST. The electrical system is comprised of two ac systems connected by a three-phase transmission line. The ST is connected at the sending end of the transmission line. Table I gives the parameters for both the ST and the network.

1) Electrical Network Model: The ac sources at both sending and receiving ends are modeled as infinite sources with the same magnitude but at a phase difference of $20°$ (the receiving end voltage lags the sending end voltage). The transmission line is modeled as a lumped series impedance.

2) ST Model: The ST is a specially designed transformer with multiple windings having multiple tap positions in the secondary. The model for such a transformer is not available in PSCAD/EMTDC. Therefore, nine single-phase transformers, each having on-load tap changing capability have been used to model the ST. By using single-phase transformers, inter-phase
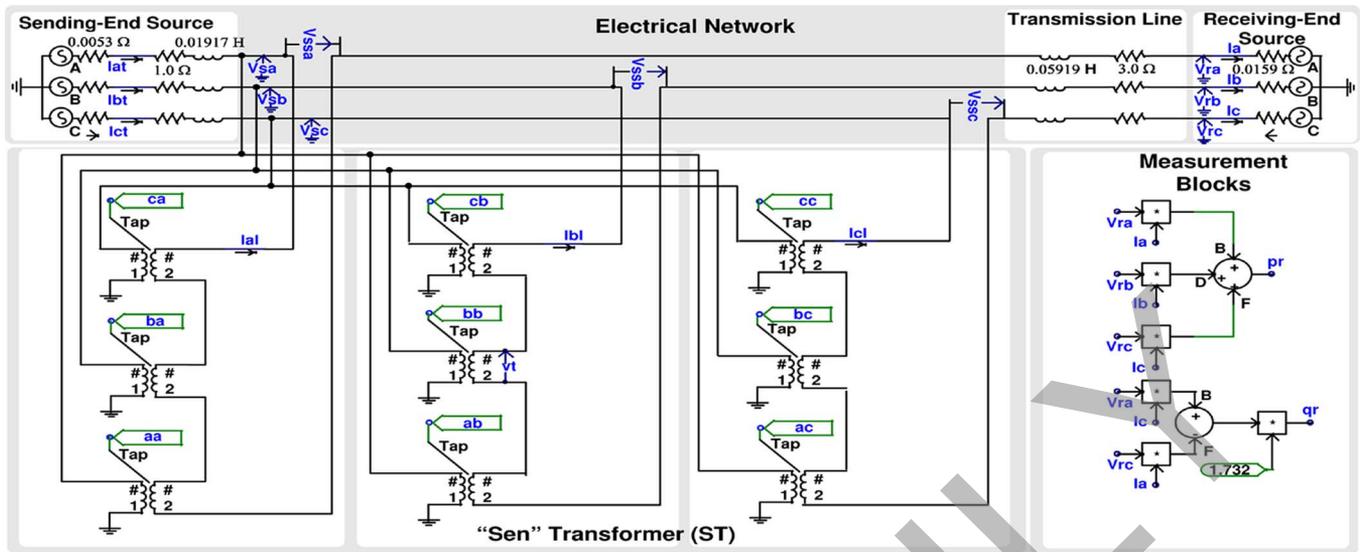
Fig. 4. Electrical network and the ST modeled in PSCAD/EMTDC.
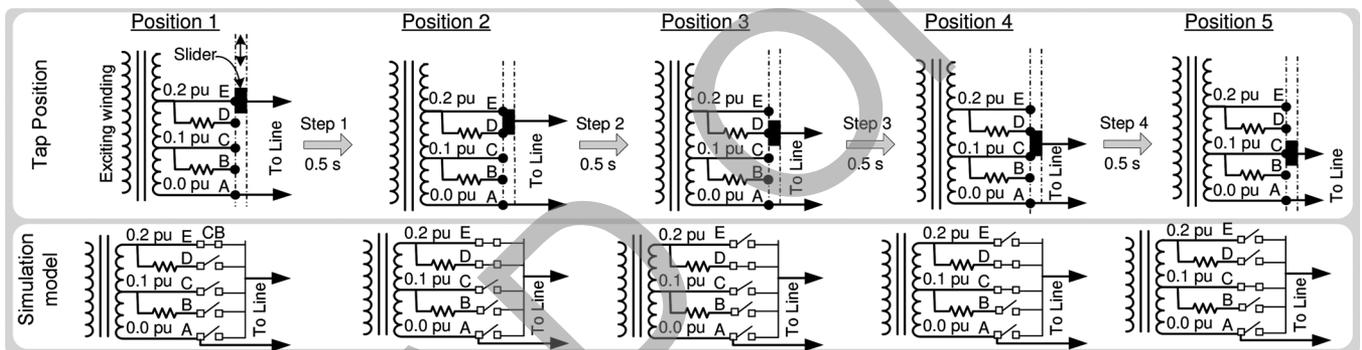
Fig. 5. Tap-changing mechanism and its model for digital simulation.

mutual flux linkage and thus mutual inductance has not been considered, which may cause some discrepancies in the results. These nine single-phase transformers are modeled with a small resistance and leakage reactance as shown in Table I. Output voltages of three transformers (contributing from phase a, b and c) are added in series and then fed to one phase of the transmission line. The nine outputs (*aa, ab, ac, ba, bb, bc, ca, cb,* and *cc*) from the tap-selection algorithm supply the value of tap setting to all nine transformer Tap terminals. Should these outputs undergo any changes, the transformers readjust their tap positions and produce the required compensating voltages.

3) Tap Changer Model: In a practical transformer, tap changing is performed through a tap selector, where a resistor or inductor is used in parallel with the tap positions to limit the current through a shorting winding segment between two consecutive taps. In Fig. 5, an example of tap-changing operation has been shown along with the equivalent PSCAD/EMTDC model for each position of the tap selector. Although, practical transformers with onload tap changers (OLTC), such as the ones from Reinhausen [8] use taps with voltage difference in the range of 0.02 p.u. to 0.067 p.u., in this model a voltage difference of 0.1 p.u. between taps has been assumed for the

clarity of simulation. The time required to move the tap selector between adjacent tap positions is 2 s [8]. In order to move the tap selector from its initial position, terminal E (0.2 p.u.) to its final position, terminal C (0.1 p.u.), the following four steps of approximately 0.5 s each are performed.

- **Step 1**: In position 1, the tap selector is connected to terminal E; therefore, in the model the circuit breaker (CB) connecting terminal E to line is closed and the rest of the CBs are open. Now, the selector is moved to a position where it connects both terminal D and E; however, the current flows through terminal E alone. To model this situation, the CB connecting terminal D is closed.
- **Step 2**: The tap selector moves further down and is connected to terminal D. The line current now flows through the resistor, and depending on the value of the resistance, a slight dip in the voltage may occur. In the model, CB connecting terminal E is opened.
- **Step 3**: In this step, the tap selector is moved to a position, where it connects both terminals C and D. This is the situation where a circulating current will flow within the loop formed by the terminals C, D and the resistor. The higher the value of the resistor, the lower will be the cir-
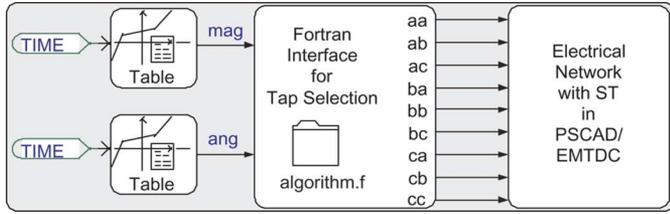
Fig. 6. Interfacing of the ST control system with the electrical system in PSCAD/EMTDC.

Fig. 7. P_r and Q_r of the ST and the UPFC with $V_{s's} = 0.4$ p.u. at a varying phase angle (β).

culating current, however, too high a value of resistance would cause a voltage sag. In the model, the CB connecting terminal C is now closed.

- **Step 4**: In the final step, the tap selector is moved to allow contact with terminal C alone, which is the required final position. In the model, the CB connecting terminal D is opened.

4) Measurements: Measurement blocks are used to measure electrical signals and, hence, to calculate powers at the receiving end using the following equations:

$$P_r = (v_a i_a + v_b i_b + v_c i_c) \qquad (4)$$
$$Q_r = \sqrt{3}(v_a i_c - v_c i_a) \qquad (5)$$

where v_a, v_b, and v_c are the voltages of phase a, b and c, respectively, and i_a, i_b, and i_c are the currents in the respective phases.

B. Tap-Selection Algorithm Implementation

The tap-selection algorithm has been implemented as a FORTRAN program linked to the electrical system using an interfacing block (Fig. 6) created in PSCAD/EMTDC. Although PSCAD/EMTDC has the capability of interfacing other scripts such as MATLAB, C or $C++$, FORTRAN has been chosen for its simplicity and the speed of implementation. The input to the interfacing block are the magnitude ($V_{s's}$) and the phase angle (β) of the compensating voltage and the outputs are the tap positions for the nine compensating windings of the ST. Any change in the demand of series voltage is passed to the FORTRAN program which implements the tap selection algorithm (described in Section III) and then determines the necessary tap positions which are sent to the electrical system and implemented through the on-load tap changer of the transformer.

In Fig. 6, a Time block has been used to synchronize the instant of inputs ($V_{s's}$ and β) with the simulation time. Two Table blocks have been introduced to serve the purpose of a lookup table. The inputs which vary with respect to time, can be predefined through these blocks for both $V_{s's}$ and β. Based on these inputs, the tap-selection program produces the value of tap ratio through the outputs *aa, ab, ac, ba, bb, bc, ca, cb,* and *cc*. The first letter of the output variable (for example, *aa*) denotes the contributing phase and the second letter indicates the phase in which the voltage is added in series. These outputs are then passed to the compensating transformers for the readjustment of tap setting.
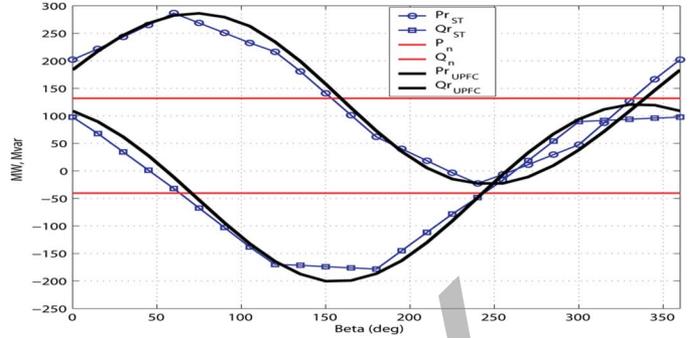
IV. SIMULATION CASE STUDIES

Before injecting any series voltage ($V_{s's}$), the system has been simulated in an uncompensated mode with the network parameters listed in Table I. The equations used for the calculation of active and reactive power at the receiving end, are given in (4) and (5). The results are compared between the ST where PSCAD/EMTDC is used as the simulation tool and the proposed algorithm is interfaced through a FORTRAN program, and the UPFC using ATP simulation where voltage-source converters (VSC) are modeled as controllable sinusoidal voltage sources at the fundamental frequency. In an uncompensated mode, P_r and Q_r become natural power flows and are denoted by P_n and Q_n, respectively. In the compensated mode, with an ST rating of 10 MVA/phase, the following cases have been simulated.

- Case I: Steady-state performance of the ST when β is varied between 0° and 360° while $V_{s's}$ is kept to value between 0.1 to 0.4 p.u with a step of 0.1 p.u.
- Case II: Transient Response of the ST showing step-response of active and reactive power demand.

A. Case I

Simulation of a compensating series voltage of 0.1 p.u. to 0.4 p.u. was performed at different β for both the ST and the UPFC. The angle β was varied at a discrete step of 15° in the range of 0° to 360°. The variation of both P_r and Q_r for $V_{s's} = 0.4$ p.u. are shown in Fig. 7 where the ST is found to follow the UPFC quite closely. For the ST, the maximum and minimum P_r are +286.69 MW and −22.73 MW. A negative active power indicates the reversal of power flow. The injected series voltage changes natural active power flow, P_n, by +154.77 MW and −154.65 MW. The level of reactive power flow is increased and reached to a maximum of +97.80 Mvar and a minimum of −178.3 Mvar, which changed the natural reactive power flow Q_n by +138.2 Mvar and −137.9 Mvar, respectively. It is interesting to note that both active and reactive power change equally in both directions.

Almost similar results were found for the UPFC. The peaks of the active power flow using the UPFC reaches to +286.3 MW and −22.21 MW and for reactive power flow, they are +120.55 Mvar and −200.4 Mvar, respectively. This gives a maximum deviation of P_r from its natural power flow
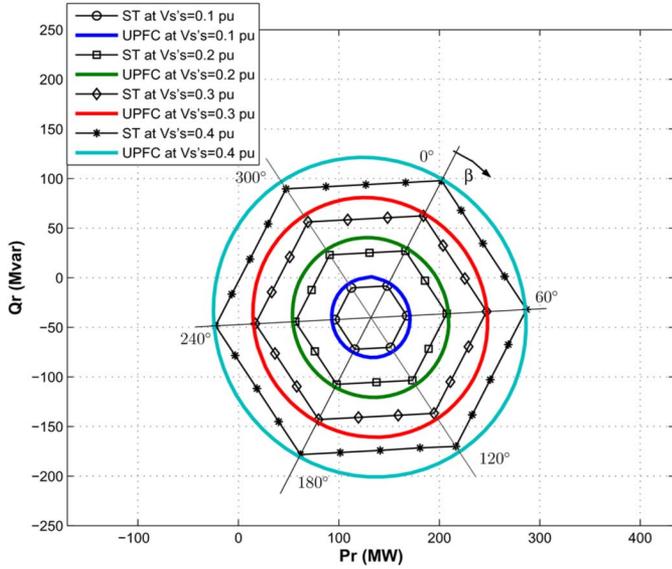
Fig. 8. Relationship between P_r and Q_r at various phase angle β and series voltage $V_{s's}$ for the ST and the UPFC.

P_n by $+154.38$ MW and -154.73 MW, respectively. Similarly, Q_r also follows a sinusoidal pattern with an amplitude of $+160.95$ Mvar and -160.0 Mvar, respectively. The variation of power flow using the UPFC is fully sinusoidal but for the ST, it is almost a first-order-hold sinusoidal pattern. The ST power-flow variation is linear with β but split into six regions with different slopes. In the range of $\beta = 120°$ to $180°$ and $\beta = 300°$ to $360°$, Q_r shows very little or no change in its value. This can be explained with the help of (2) by substituting V_s and δ with $V_{s'}$ and δ', respectively, when Q_r becomes a function of $V_{s'}$ and $\cos\delta'$. In the range of $\beta = 120°$ to $180°$, $V_{s'}$ decreases whereas $\cos\delta'$ increases and the net change of Q_r becomes very little or negligible. The opposite phenomenon occurs for $\beta = 300°$ to $360°$ (i.e., $V_{s'}$ increases but $\cos\delta'$ decreases and results in negligible changes in Q_r).

The relationship between P_r and Q_r for $V_{s's}$ of 0.1 p.u., 0.2 p.u., 0.3 p.u., and 0.4 p.u. is shown in Fig. 8 for both the UPFC and the ST. It has been found that the ST produces a hexagon profile whereas the UPFC produces a circular profile. The following items highlight the differences between the two power-flow profiles.

- At six points on the profiles, both P_r and Q_r for the UPFC and the ST are almost the same; however, the path between these points is different for the ST and the UPFC. For the ST, the path is linear whereas for the UPFC, it is an arc. These six points are found to be at $\beta = 0°$, $60°$, $120°$, $180°$, $240°$, and $300°$. Only at these points, the ST produces a series voltage injection with zero error (i.e., $\varepsilon_k = 0$) and the injected voltage is exactly equal to the required series voltage, $V_{s's}$. At angles, $\beta = 0°$, $120°$, and $240°$, the series voltage is supplied by only one compensating winding, while at $\beta = 60°$, $180°$, and $300°$, voltages are contributed equally from two different phases. For example, if $V_{s's} = 0.4$ p.u. is required at $\beta = 180°$ in phase a, the voltage would be supplied by both phase b and phase c, each with a 0.4-p.u. injection. The result of these two

contributing voltages is exactly equal to 0.4 p.u. at an angle of $180°$ with respect to phase a, thereby making $\varepsilon_k = 0$.

- The P_r versus Q_r plot for the UPFC is smooth circular because it is capable of producing any series voltage at any angle and the variation of power flow with β is sinusoidal. The circular control region of a UPFC can be explained with the following boundary equation [1]:

$$[P_r(\beta) - P_n]^2 + [Q_r(\beta) - Q_n]^2 = \left[\frac{V_r V_{s's}}{X_L}\right]^2 \quad (6)$$

where the center of the circle lies at P_n and Q_n and $V_r V_{s's}/X_L$ is the radius. On the other hand, the ST produces a hexagon profile due to the three-phase voltage summation. Unlike the UPFC, in most cases, the ST does not produce the exact amount of required series voltage at exact angle (i.e., $\varepsilon_k \neq 0$).

- The ST profile is enclosed within the UPFC profile indicating that the ST produces a little less power than the UPFC, except at the six corner points where they are almost equal.

The simulation results are in excellent agreement which corroborates the fact that the ST can be a good alternative power-flow controller where tap changer's response time is sufficient.

B. Case II

In this case, the transient responses of the ST and the UPFC have been studied through various preset series voltage injections. Fig. 9 shows P_r and Q_r for the ST and the UPFC. The system has been simulated as an uncompensated line until $t = 5$ s when a compensating voltage of 0.2 p.u. at a leading angle of $120°$ is inserted in series. At the beginning, a power flow of $P_n = +131.92$ MW and $Q_n = -40.22$ Mvar for the ST and $P_n = +131.91$ MW and $Q_n = -40.21$ Mvar for the UPFC have been found in uncompensated mode. With the insertion of $V_{s's} = 0.2$-p.u. series voltage at a leading angle of $\beta = 120°$ at $t = 5$ s, a change in P_r and Q_r has been observed and both settled to new power levels such as $P_r = +85.4$ MW and $Q_r = +24.92$ Mvar for the ST and $P_r = +84.6$ MW and $Q_r = +25.73$ Mvar for the UPFC, respectively. It is interesting to note that the reactive power flow became positive (inductive). For the UPFC, the calculation for the required compensating voltage is performed within one sampling time of the microprocessor, but the implementation takes place through a 1-s ramp [9]. Fig. 9 shows the ramp variation of power-flow changes for the UPFC. However, for the ST, the response is step-wise and follows the tap changing mechanism that took place between $t = 5$ s to $t = 9$ s (4-s duration) when the tap-to-tap voltage is considered to be 10% of the rated voltage. If the transformer taps are less than 10%, the ST will take more time to reach to its required tap-position. For example, a 0.2-p.u. voltage injection with 1% tap will take 10 times longer (i.e., 40 s to complete the tap-changing operation).

In Fig. 9, the power flow remains uninterrupted until $t = 14$ s when β is changed to $60°$, keeping the $V_{s's}$ at 0.2 p.u. Similar transient responses have been observed and the new power levels are $P_r = +53.95$ MW and $Q_r = -45.8$ Mvar for the ST and $P_r = +54.3$ MW and $Q_r = -46.81$ Mvar for the
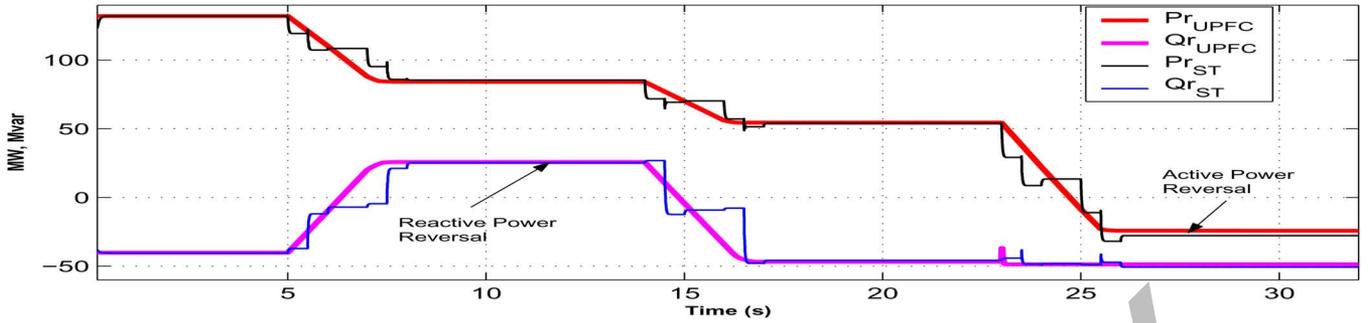
Fig. 9. Transient response of P_r and Q_r of the ST and the UPFC. (Natural power flows until $t = 5$ s, $V_{s's a} = 0.2$ p.u. at $\beta = 120°$ injected at $t = 5$ s, $V_{s's a} = 0.2$ p.u. at $\beta = 60°$ injected at $t = 14$ s and $V_{s's a} = 0.4$ p.u. at $\beta = 60°$ injected at $t = 23$ s.
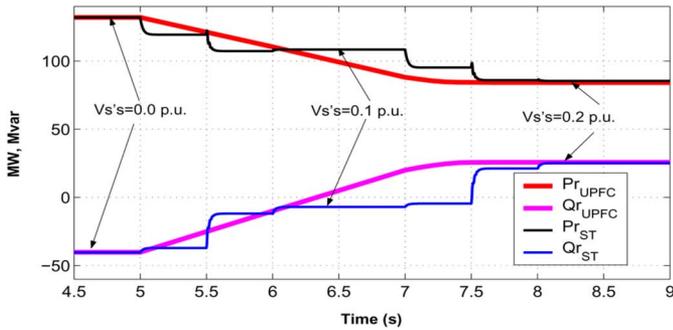
Fig. 10. Zoomed view of P_r and Q_r, while $V_{s's} = 0.2$ p.u. at $\beta = 120°$ is injected at $t = 5$ s.

Fig. 11. Profile of injected series voltage $V_{s's a}$ and line current Ia by the UPFC and the ST: $V_{s's a} = 0$ at $\beta = 0$ for $t < 5$ s, $V_{s's a} = 0.2$ p.u. at $\beta = 120°$ for 5 s $< t < 14$ s, $V_{s's a} = 0.2$ p.u. at $\beta = 60°$ for 14 s $< t < 23$ s and $V_{s's a} = 0.4$ p.u. at $\beta = 60°$ for 23 s $< t < 32$ s.

UPFC. The results are in close conformity and as expected, the ST goes through the tap changing steps and settles to its final value. The next change in series voltage injection is imposed at $t = 23$ s when $V_{s's}$ is changed to 0.4 p.u. at $\beta = 60°$. This forced the power levels to shift to $P_r = -27.82$ MW and $Q_r = -50.8$ Mvar for the ST and to $P_r = -24.21$ MW and $Q_r = -48.6$ Mvar for the UPFC. A negative power flow can be observed which indicates the reversal of power flow in the line.

Fig. 10 shows the zoomed view of power transitions for both the ST and the UPFC due to a series voltage injection of 0.2 p.u. at $\beta = 120°$. The series voltage injection at $t = 5$ s caused the tap selector of *ab*, *bc* and *ca* to change to 0.2 p.u. from its previous position of 0.0 p.u. through multiple steps as described in Section IV. Generally, a duration of 2 s is required for the tap selector to move from 0.0 p.u. to 0.1 p.u. [8] (through four steps of 0.5 s); therefore, a total of 4 s transition time is allowed for the tap selector to move from 0.0 p.u. to 0.2 p.u. Between 5 s $< t \leq 5.5$ s, the tap selector is connected in parallel with terminal A and B (Fig. 5), causing a circulating current to flow between the terminals and, hence, reducing both $V_{s's}$ and the load current. This causes reductions in power levels as observed in Fig. 10. Between 5.5 s $< t \leq 6.0$ s, the tap selector moves to terminal B only. Terminal B injects slightly less voltage than 0.1 p.u. as it is connected through a bypass resistor. This causes a significant change in the value of $V_{s's}$, P_r, and Q_r. Between 6.0 s $< t \leq 6.5$ s, the tap selector goes in parallel with terminal B and C which causes negligible or no changes in the $V_{s's}$ and power levels. In the next step, between 6.5 s $< t \leq 7.0$ s, the tap selector is connected to terminal C only. At this position, the tap selector injects 0.1 p.u. and the changes in $V_{s's}$, P_r and
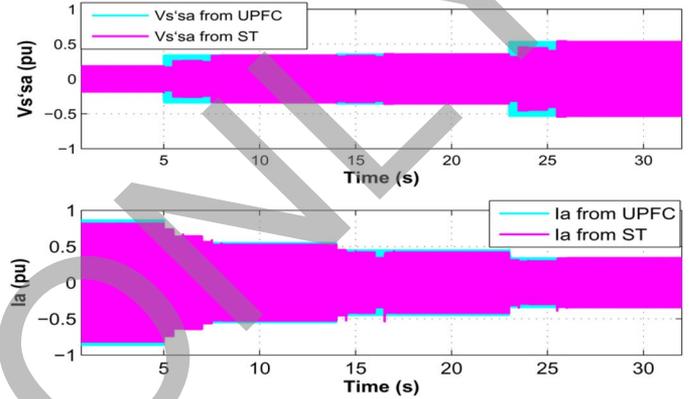
Q_r are minimum. Similarly, in the next 2.0 s, between 7 s $< t \leq 9$ s, the tap selector reaches to its final position of 0.2 p.u. Each change of the tap selector's position produces changes in the power levels of the ST as observed in Fig. 10.

The profile of the injected series voltage $V_{s's a}$ and the line current I_a for both the ST and the UPFC are shown in Fig. 11. It is clear that both $V_{s's a}$ and I_a for the ST and the UPFC maintains the same profile except for the transition periods when the ST injects voltage in multiple steps. This case study indicates that P_r and Q_r for both the ST and the UPFC are in close agreement. Also, it is observed that when reference levels are changed, both the UPFC and the ST experiences the same changes in power levels, which establishes the fact that the ST can provide the same power-flow control functionalities as the UPFC. The reversal of both active and reactive power can also be achieved by using the ST as it is possible by the UPFC. The only difference in their performance is in their response time. The dynamic performance of an ST can be in the half-cycle range of power frequency if electronic taps are used. It can also be in a minute range if mechanical tap changers are used. Even though the UPFC can respond in less than a half-cycle range of power frequency, currently installed UPFCs are designed to respond in seconds for power-flow control applications [7]. All case studies demonstrate the effectiveness of the proposed tap-selection algorithm applied to the ST. Minor discrepancies in the simulation results can be attributed to the differences in the modeling details of the two devices.

In the simulation, balanced power system conditions were assumed. Therefore, there were no second harmonics in the power calculation. However, in a realistic power system with unbalanced voltages and/or currents, the second harmonic component will be superimposed on the dc component when power is calculated using (4) and (5). A simple remedy to overcome the effect is to filter the measured quantities using a half-cycle window averager.

In this paper, a 30-MVA ST was selected for a 160-MVA power system with a maximum voltage injection of 0.4 p.u. and 10% taps. While the chosen ST rating may not be typical, it shows the wide capability of the ST, especially, the power reversal. The rating selection method for the ST is similar to that of a UPFC. The factors that need to be considered for selecting the ST rating include network parameters, location of the ST and the purpose of the ST (voltage regulation, line impedance, or phase angle control).

V. CONCLUSION

This paper proposes a novel algorithm for the selection of tap setting for the "Sen" transformer. The algorithm has been implemented in digital simulation model of the ST using PSCAD/EMTDC package through an interface with FORTRAN program. The tap-selection algorithm is simple but effective, and can be easily implemented on an inexpensive DSP or microcontroller. A comparative study of the ST and the UPFC under different operating conditions has revealed the following items.

- The ST is an effective power-flow controller with an acceptable response time in most utility applications with presently available mechanical tap changers.
- The UPFC can be a fast power-flow controller with a response time less than a half cycle of the power frequency; however, the response time of the currently installed UPFCs are adjusted to operate in the range of seconds.
- The ST uses traditional components such as transformers and tap changers whereas the UPFC uses power-electronic-based technology which requires high installation and operating costs. Therefore, the ST is an economical and effective alternative to the UPFC.
- The implementation of the tap-selection algorithm for the ST is much easier and economical in comparison to the UPFC control implementation.

REFERENCES

[1] N. G. Hingorani and L. Gyugyi, *Understanding FACTS- Concept and Technology of Flexible AC Transmission Systems*. Piscataway, NJ: IEEE Press, 2000.

[2] B. A. Renz, A. Keri, A. S. Mehraban, C. Schauder, E. Stacey, L. Kovalsky, L. Gyugyi, and A. Edris, "AEP unified power flow controller performance," *IEEE Trans. Power Del.*, vol. 14, no. 4, pp. 1374–1381, Oct. 1999.

[3] K. K. Sen and E. J. Stacey, "UPFC-unified power flow controller: Theory, modeling and applications," *IEEE Trans. Power Del.*, vol. 13, no. 4, pp. 1453–1460, Oct. 1998.

[4] E. J. Stacey and M. B. Brennen, "Active Power Conditioner System," U.S. 4651265, 1987.

[5] M. B. Brennen and B. Banerjee, "Low cost high performance active power line conditioners," in *Proc. 3rd Int. Conf. Power Quality: End-Use Applications and Perspectives, EPRI*, Amsterdam, The Netherlands, 1994.

[6] K. K. Sen and M. L. Sen, "Introducing the family of "sen" transformers: A set of power flow controlling transformers," *IEEE Trans. Power Del.*, vol. 18, no. 1, pp. 149–157, Jan. 2003.

[7] K. K. Sen and M. L. Sen, "Comparison of the sen transformer with the unified power flow controller," *IEEE Trans. Power Del.*, vol. 18, no. 4, pp. 1523–1533, Oct. 2003.

[8] *"Load Tap Changer, Type RMV-A,"* Reinhausen Manufacturing, instruction manual, TL 8001.01.

[9] K. K. Sen and A. J. F. Keri, "Comparison of field results and digital simulation results of voltage-sourced converter-based facts controllers," *IEEE Trans. Power Del.*, vol. 18, no. 1, pp. 300–306, Jan. 2003.

M. Omar Faruque (S'03) received the B.Sc.Engg. degree from Chittagong University of Engineering and Technology (CUET), Bangladesh, in 1992 and the M.Eng.Sc. degree from the University of Malaya, Malaysia, in 1999. He is currently pursuing the Ph.D. degree in the Department of Electrical and Computer Engineering, University of Alberta, Edmonton, AB, Canada.

He has worked in both industry and academia and his research interests include FACTS, HVDC, and real-time digital simulation and control of power electronics and power systems.

Venkata Dinavahi (M'00) received the Ph.D. degree in electrical and computer engineering from the University of Toronto, Toronto, ON, Canada, in 2000.

Currently, he is an Associate Professor with the University of Alberta, Edmonton, AB, Canada. His research interests include electromagnetic transient analysis, power electronics, and real-time simulation and control.